Solvent-Free Fabrication of Flexible and Robust Superhydrophobic Composite Films with Hierarchical Micro/Nanostructures and Durable Self-Cleaning Functionality

Liu, Shanqiu ; Zhang, Xiaotian ; Seeger, Stefan

Abstract: Superhydrophobic surfaces hold tremendous potential in a wide range of applications owing to their multifaced functionalities. However, the mechanochemical susceptibility of such materials hinders their widespread usage in practical applications. Here, we present a simple, solvent-free, and environmentally friendly approach to fabricate flexible and robust superhydrophobic composite films with durable self-cleaning functionality. The obtained composite film features unexpected but surprising hierarchical micro/nanoscopic structures as well as robust superhydrophobicity with a water contact angle of similar to 170 degrees and a sliding angle below 4 degrees. Notably, the composite film exhibits mechanical robustness under cyclic abrasion, tape peeling, flexing, intensive finger wiping, and knife cutting; maintains excellent superhydrophobicity after long-time exposure to a high-humidity environment; and sustains exposure to highly corrosive species, such as strong acid/base solutions and organic solvents. The robust superhydrophobicity is ascribed to the induced micro/ nanohierarchical surface structures, resulting in the trapped dual-scale air pockets, which could largely reduce the solid/liquid interface. In addition, even after oil contamination, the composite film water repellency and self-cleaning functionality. The robust superhydrophobic composite film developed here is expected extend the application scope of superhydrophobic materials and should find potential usage in various industries and daily life.

DOI: https://doi.org/10.1021/acsami.9b15318

Solvent-free Fabrication of Flexible and Robust Superhydrophobic Composite Films with Hierarchical Micro-/Nanostructures and Durable Self-cleaning Functionality

*Shanqiu Liu‡, Xiaotian Zhang‡, and Stefan Seeger**

Department of Chemistry, University of Zurich, Winterthurerstrasse 190, CH-8057 Zurich, Switzerland.

KEYWORDS: solvent-free fabrication, nanofilaments, robust superhydrophobicity, hierarchical micro/nano structures, durable self-cleaning

ABSTRACT: Superhydrophobic surfaces hold tremendous potential in a wide range of applications owing to their multifaced functionalities. However, the mechanochemical susceptibility of such materials hinders their widespread usage in practical applications. Here, we present a simple, solvent-free and environmentally friendly approach to fabricate flexible and robust superhydrophobic composite films with durable self-cleaning functionality. The obtained composite film features unexpected but surprising hierarchical micro/nanoscopic structures as well as robust superhydrophobicity with water contact angle around 170° and sliding angle below 4°. Notably, the composite film exhibits mechanical robustness under cyclic abrasion, tape-peeling,

flexing as well as intensive finger wiping and knife-cutting, maintains excellent superhydrophobicity after long time exposure to high humidity environment, as well as sustains exposure to highly corrosive species, such as strong acid/base solutions and organic solvents. The robust superhydrophobicity is ascribed to the induced micro/nano hierarchical surface structures, resulting in the trapped dual-scale air pockets which could largely reduce the solid/liquid interface. In addition, even after oil contamination, the composite film maintains its water repellency and self-cleaning functionality. The robust superhydrophobic composite film developed here is expected to extend the application scope of superhydrophobic materials and should find potential usage in various industries and daily life.

INTRODUCTION

Superhydrophobic surfaces have drawn great interest in both academia and industry due to their great potential in numerous applications, such as self-cleaning,[1-5] water proofing,[6] anti-icing[7], -corrosion[8], and -bacterial[9, 10], drug release and delivery[11, 12], water-oil separation,[13-21] low-friction transport of fluids[22] as well as droplet manipulation[23-26]. Provoked by these attractive multifaceted functionalities, various techniques have been developed to fabricate surfaces with non-wetting properties including spray coating[27], vapor deposition[28-31], lithography[32], chemical etching, [33, 34] electro-spinning, self-assembly, etc.[35, 36] The general synthesis strategy of water repellent surfaces is to introduce the micro/nanostructured roughness followed by chemical modification to generate a low-energy surface.[37] Although the successful fabrication of superhydrophobic surfaces have been widely reported, the mechanical susceptibility severely limits their widespread usage in practical applications.[38] Mechanical treatment, such as abrasion or scratching applied on the substrate surface can easily render the loss of superhydrophobicity, because mechanical contacts

lead to the destructions of the micro/nanoscale surface structures which is essential to sustain the non-wetting property.

To overcome this issue, fabrication of mechanically durable surfaces featuring non-wetting property has recently been explored extensively. A commonly adapted strategy is to create superhydrophobic surfaces based on substrates that are inherently mechanical robust, such as elastomers and metals. For instance, Zhong and co-workers[39] reported the fabrication of superhydrophobic polydimethylsiloxane films by a duplication process based on a Femtosecond Laser Ablated Template. Tan and co-workers[40] constructed micro–nanostructure on the brass surface via micro-etching technique, followed by surface modification with stearic acid to render the surface superhydrophobic. Wang and co-workers[41] prepared a superhydrophobic steel surface using hydrogen peroxide and acid for etching to obtain hierarchical structured surface on the steel, followed by a surface modification treatment. Although the superhydrophobic surfaces demonstrated in these works exhibited good mechanical durability, these strategies suffer from costly and complicated production which limits their applicability. As an alternative solution, spray coating of hydrophobized particles (*e.g.*, fluorinated nanoparticles) along with adhesives has been widely used to prepare mechanical durable superhydrophobic surfaces due to its relatively uncomplicated implantation. For instance, Tiwari and co-workers[42] presented a multi-fluorination strategy to prepare robust superhydrophobic surfaces by spray coating the mixture of fluorinated epoxy resin and polytetrafluoroethylene nanoparticles dispersed in acetone. The authors demonstrated that the obtained superhydrophobic coating exhibited good mechanical durability and water impalement resistance. Parkin and co-workers reported that spray coating of perfluoro silane modified titanium dioxide nanoparticles on adhesive tapes resulted in a superhydrophobic surface that shows good mechanical stability.[43] However, the fluorinated substances and organic

solvents that involved in these spraying methods are not environmental friendly and involve safety concerns. In addition, the superhydrophobic surfaces generated by these spraying methods normally feature chemical instability when exposed to organic solvents. As such, fabrication of mechanochemically robust superhydrophobic surface via a simple eco-friendly way is very appealing but remains challenge.

Here, we report a facile solvent-free method to fabricate flexible superhydrophobic composite films that feature novel hierarchical micro/nanoscale surface structures and mechanochemically robust superhydrophobicity. Unlike most spraying techniques, this strategy avoids the usage of solvents, especially organic solvents, which reduces the cost as well as environmental and safety concerns. The robust superhydrophobic composite film was generated by coating silicone nanofilaments (SNF) on a plasma activated polyethylene (PE) film through the *droplet-assisted growth and shaping* (DAGS) method[44], followed by thermal annealing of the composite film at 180 °C for 10 min. Strikingly, after thermal treatment the as-prepared film exhibited hierarchical micro/nanoscale surface structures, leading to the excellent water repellency due to the trapped dual-scale air pockets within the induced hierarchical structures. Moreover, the obtained composite film possessed mechanically robust superhydrophobicity under cyclic abrasion, tape-peeling, flexing, as well as intensive finger wiping and knife-cutting, and maintained its excellent water repellency even after exposure to highly corrosive liquids, such as strong acid/base solutions and organic solvents. Notably, even after oil contamination the composite film can retain its water repellency and self-cleaning functionality. The superhydrophobic composite film developed here shows great potential and advantageous for various applications that require a stable and robust superhydrophobicity.

RESULTS AND DISCUSSION

Figure 1a schematically shows the preparation of the superhydrophobic composite film with hierarchical micro/nanoscale surface structures. The dense and homogeneous growth of silicon nanofilaments (SNF) on both side of a plasma activated polyethylene (PE) film was achieved at room temperature (RT) by the DAGS method[44] with trichloroethylsilane as precursor. The formation of silicone nanofilaments can be explained as following:[44] In a humid environment, nano- and microsized water droplets are formed on the activated PE film surface instead of forming a thin homogenous water layer, due to the topographic or chemical inhomogeneity of the substrate surface.[45, 46] After injection of the volatile trichloroethylsilane, the reaction is initiated and these small water droplets act as the "reaction vessels" throughout the reaction. The gaseous trichlorosilane reacts with water droplets to produce soluble mono and poly-silanols as well as hydrochloric acid as a by-product. The silanol and siloxanol species are produced by the hydrolysis and condensation reaction. Subsequently, polysiloxanes are formed as a result of condensation, followed by deposition as solid at the liquid-solid interface due to its insolubility in the "reaction vessel". This leads to the solid bulk grow in a 1D structure supporting the water "reaction vessel" at its tip.[44] As the activity of water droplets decreases, more gaseous water molecules are transported from the humid environment to sustain the hydrolysis and condensation reaction. Under certain circumstances, a thin silicone layer might also be formed around the water droplets due to the separation of polysiloxanes. The obtained composite film was then annealed at 180 °C for 10 min.

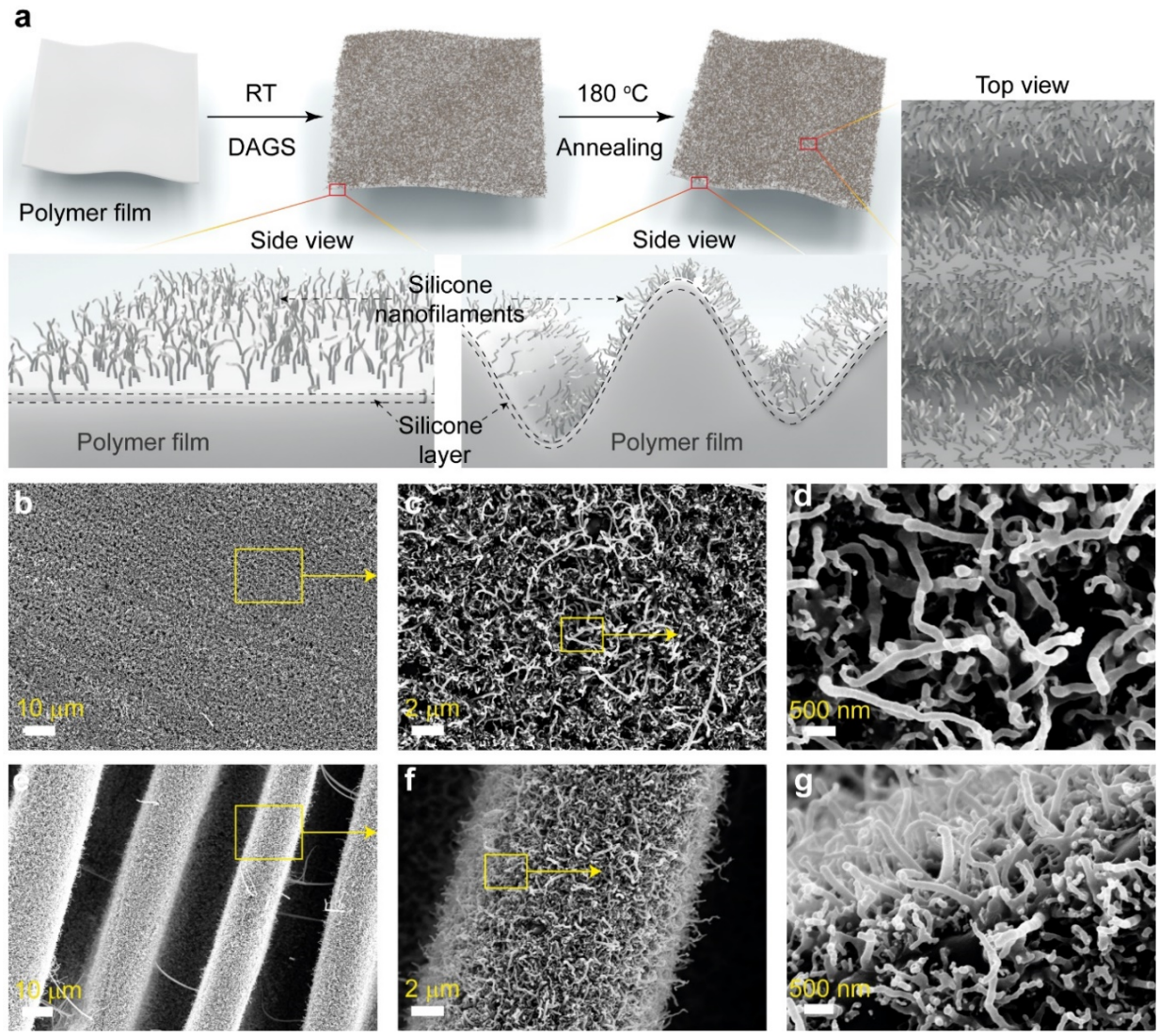

Figure 1. (a) Schematic of the strategy for sample preparation. Scanning electron microscopy (SEM) images showing the micro/nanostructure of the sample (b-d) before annealing and (e-g) after annealing at different magnifications. The annealing temperature and time were 180 °C and 10 min, respectively.

Figure 1b-d shows the scanning electron microscopy (SEM) images of the PE film after growing with SNF (PE-SNF), and a dense layer of SNF can be clearly observed on the film surface. Notably, after thermal treatment the annealed composite film (PE-SNF-A) features hierarchical micro/nanoscale surface structures, as shown in Figure 1e-g. The appeared micro-wrinkles after

annealing are ascribed to the different modulus between the thermoplastic PE film and the rigid silicon layer presented on the PE surface after growing with SNF (see Figure 1a).[47, 48]

The presence of the silicon layer on PE film surface was confirmed by the Scanning electron microscopy (SEM) and Energy-dispersive X-ray spectroscopy (EDX) images of cross-sectioned PE-SNF films, as shown in Figure 2. A thin silicon layer between PE film and the SNF can be clearly observed (Figure 2c, f, i and l). To evaluate surface roughness of the PE-SNF-A film, the height of the micro-wrinkles and the thickness of the SNF layer were determined with SEM and estimated to be ~ 19 μm and ~ 1.5 μm, respectively (Figure 2a and Figure S1). For comparison, the same thermal annealing procedure was performed for PE films without growing of SNF, whereas no micro-wrinkled structure was observed for these annealed PE films (see Figure S1).

The obtained PE-SNF-A films exhibited excellent water repellency and simultaneously good flexibility. As shown in Figure 3a, The PE-SNF-A films exhibited a mirror-like reflective behavior when submerged in water and it maintained non-wetting after being taken out, indicating the trapped air cushion between the water and solid surface.[28] A water jet can easily bounce off the highly bended PE-SNF-A composite film surface without leaving any trace (Figure 3a), which suggests the ultra-low adhesion between the film surface and water. This is also evident from the complete bouncing of a water droplet on the solid surface (case 1, Figure 3h). Additionally, the bending properties of the obtained PE-SNF films were also determined via a three-point bending measurement. The obtained flexural stress–strain curve is shown in Figure 3b. The average flexural strength and strain at maximum force of PE-SNF-A films were determined to be around 8.1 MPa and 6.7%, respectively, which is relatively higher compared to that of the unannealed PE-SNF films (5.1 MPa and 2.1%, respectively, see Figure S2). We attribute this enhancement to the induced micro-wrinkled surface structures of the annealed film.

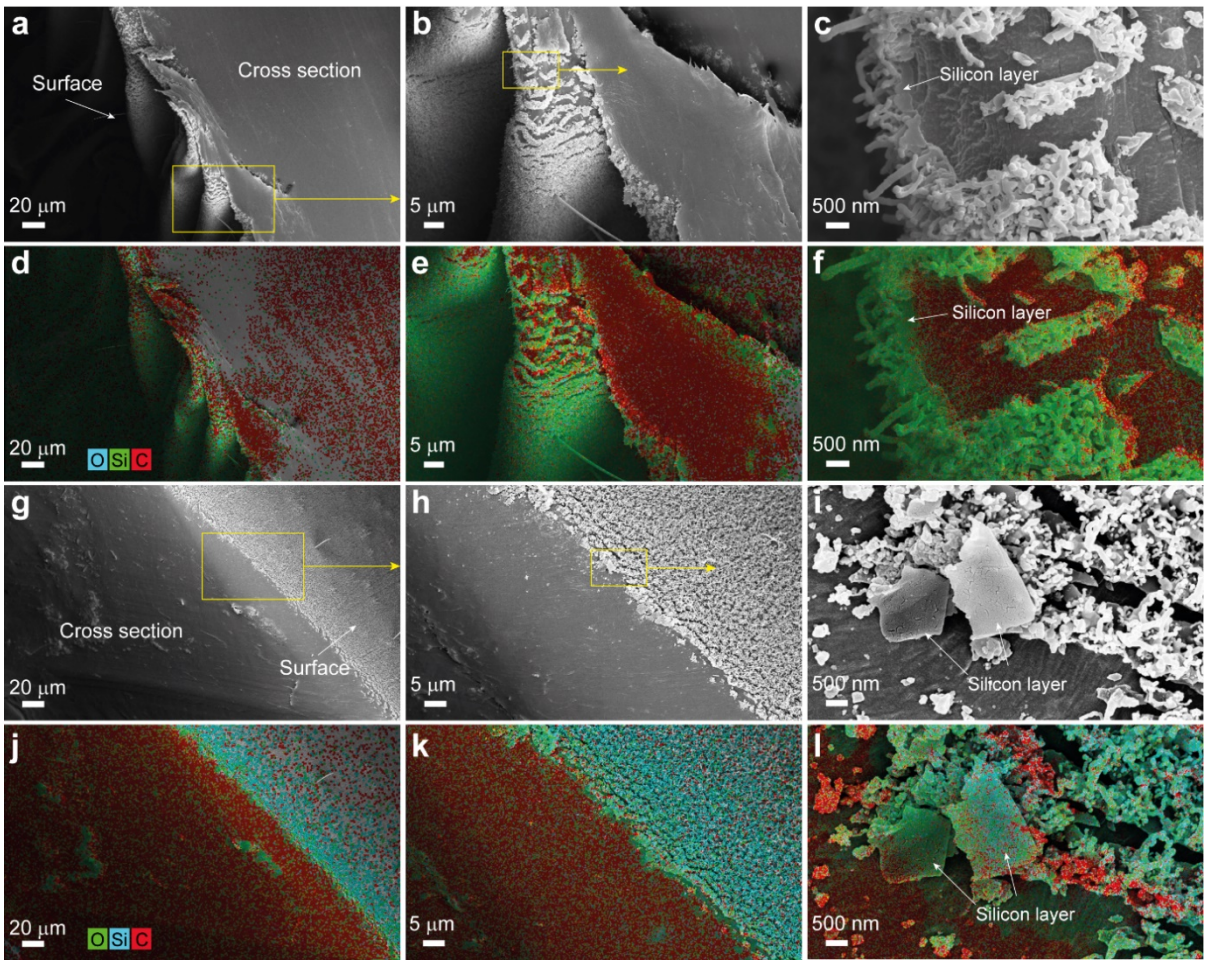

Figure 2. (a to c) SEM images of cross-sectioned PE-SNF-A film at different magnifications, and (d-f) the corresponding EDX mapping. (g to i) SEM images of cross sectioned PE-SNF film at different magnifications and (j-l) their corresponding EDX mapping.

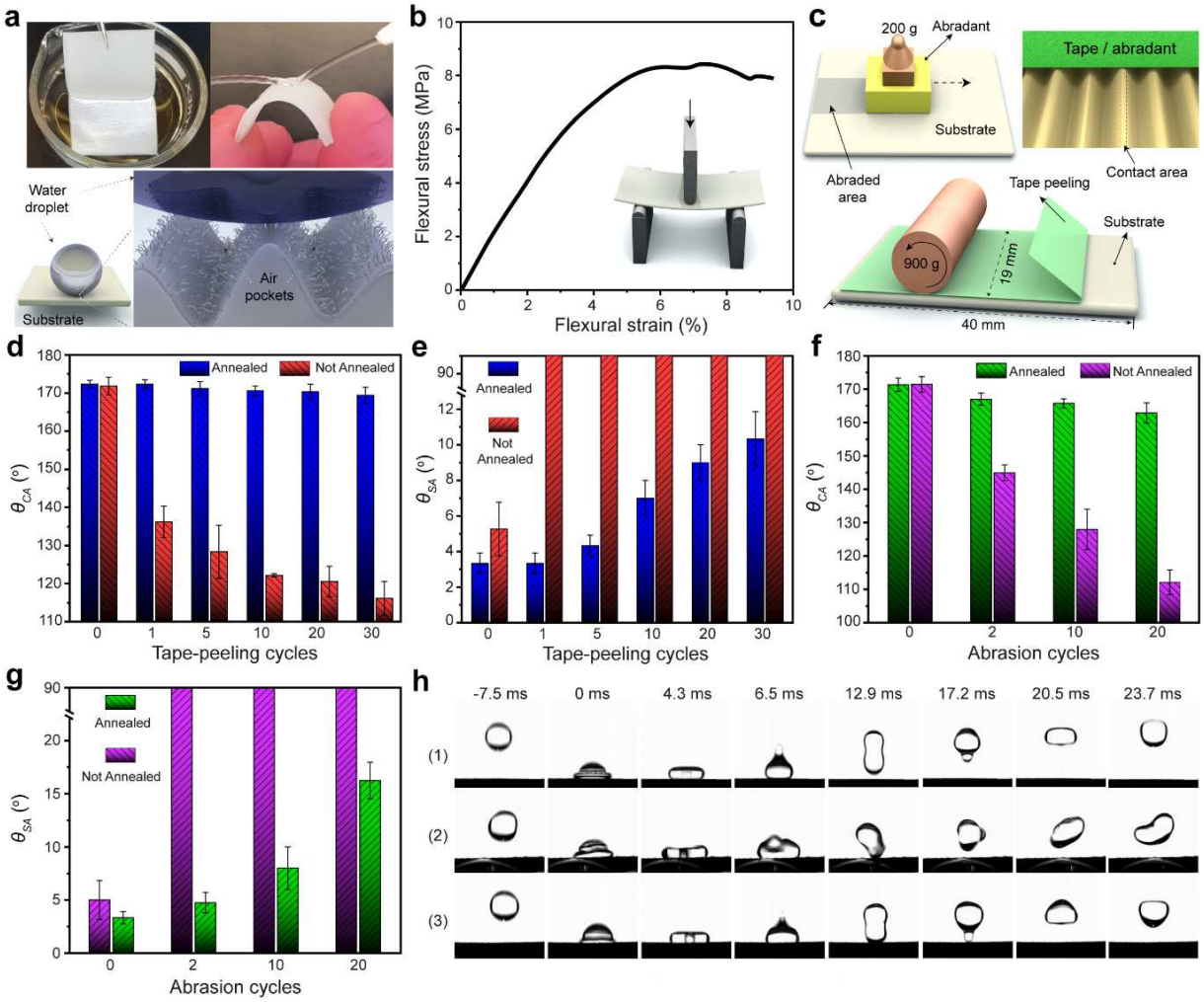

Figure 3. (a) Photos presenting the PE-SNF-A film with a mirror-like phenomenon in water and a jet bounce off the highly bended film, as well as the scheme of a water droplet on the PE-SNF-A film. (b) Flexural measurement result of the PE-SNF-A film. (c) Schematics of abrasion and tape-peeling tests. The effect of tape-peeling cycles on (d) Θ_{CA} and (e) Θ_{SA} of the composite PE-SNF films. The influence of abrasion cycles on (f) Θ_{CA} and (g) Θ_{SA} of the PE-SNF films. (h) Time resolved pictures showing the complete bounce of a 10 μL water droplet on the PE-SNF-A film (1) fresh, (2) after 30 cycles tape-peeling and (3) 20 cycles abrasion at 200 g load.

Mechanical durability is of particular importance for the practical applications of superhydrophobic materials. In this work, different types of mechanical robustness tests, *e.g.*,

abrasion and tape-peeling, were performed for the as-prepared PE-SNF composite films (see Figure 3c). For good comparison, Water contact angle (Θ_{CA}) and sliding angle (Θ_{SA}) as function of abrasion and tape-peeling cycles for both annealed and unannealed PE-SNF films were investigated. The obtained results are shown in Figure 3d-g. Both the annealed and unannealed PE-SNF films featured Θ_{CA} of around 171°, whereas the PE-SNF-A film exhibited a lower Θ_{SA} of around 3° compared to that of the PE-SNF film without annealing (Θ_{SA} of 5°). This is ascribed to the trapped dual-scale air pockets within the induced micro/nanoscale hierarchical surface structures, which can largely reduce the liquid/solid interface (see Figure 3a). Notably, the PE-SNF-A film shows a significant improvement of resistance towards tape-peeling compared to the unannealed PE-SNF film (see Figure 3d and e). Even after 30 cycles of tape-peeling, the PE-SNF-A maintained excellent superhydrophobicity featuring Θ_{CA} of above 165° and Θ_{SA} of around 10°. However, the unannealed PE-SNF film lost its superhydrophobicity quickly after only 1 round tape-peeling, and its Θ_{CA} dropped below 140° while the Θ_{SA} increased from ~ 5° to above 90°. After 30 cycles tape-peeling, the Θ_{CA} reduced to be ~ 116° for PE-SNF film without annealing (see Figure 3d).

As another mechanical durability test, the abrasion resistance of the PE-SNF films was measured. The unannealed PE-SNF film exhibited abrasion susceptibility and lost its superhydrophobicity instantly after abrasion, which is similar to the other superhydrophobic SNF coated surfaces reported previously.[38, 49] For instance, after only 2 cycles abrasion, the Θ_{CA} was reduced to be 145° and Θ_{SA} was increased to be above 90° for PE-SNF without annealing. The mechanical susceptibility of the unannealed PE-SNF film is ascribed to the inherent fragility of SNF. However, the PE-SNF-A film retained its superhydrophobicity even after 20 cycles abrasion, and its Θ_{CA} and Θ_{SA} remained around 162° and 16°, respectively, as shown in Figure 3f and g. The

mechanical robustness of PE-SNF-A film was also evidently proved by the rebounding of a water droplet on the tape-peeled (case 2, Figure 3h) and abraded (case 3, Figure 3h) surfaces. In addition, the PE-SNF-A film maintained its superhydrophobicity even after intensive finger-wiping, knife-cutting and cyclic flexing/bending (Movie S1). For instance, after 50 cycles flexing/bending the Θ_{CA} and Θ_{SA} of the PE-SNF-A film remained around 170° and 3°, respectively. However, the PE-SNF film without annealing negated its water repellency after only a few round of finger-wiping (Movie S2).

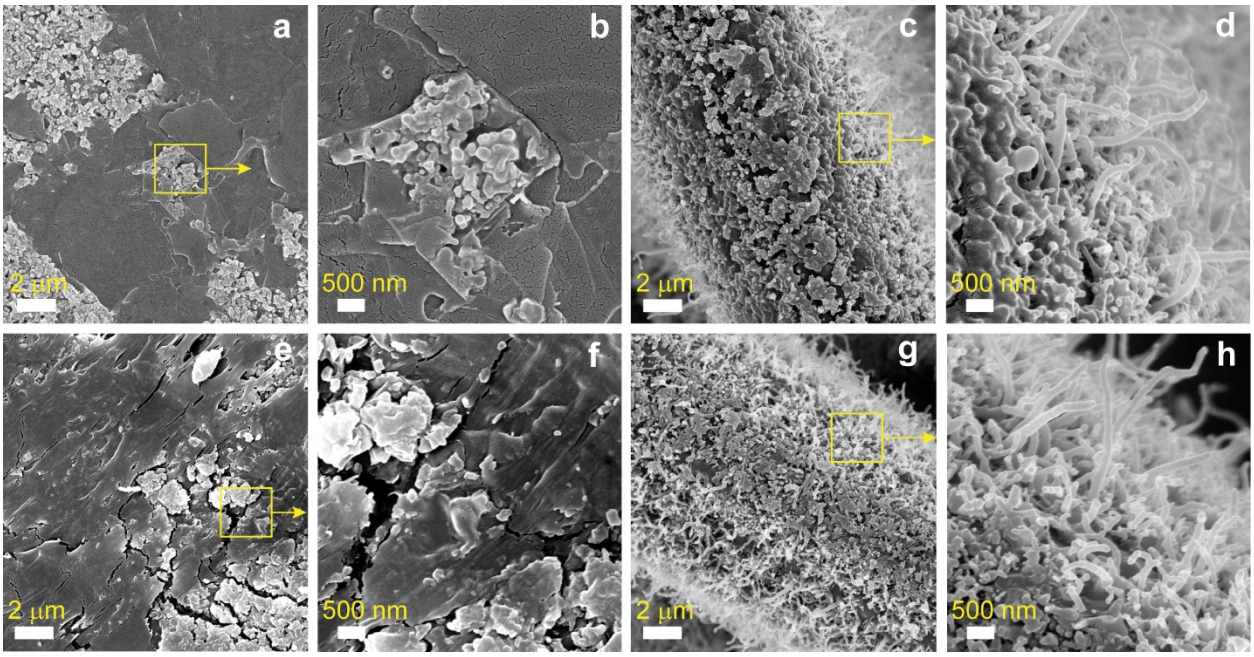

Figure 4. SEM images of the (a-b) unannealed PE-SNF and (c-d) PE-SNF-A film surfaces after 30 cycles tape-peeling at different magnifications. The (e-f) unannealed PE-SNF and (g-h) PE-SNF-A film surfaces after 20 cycles abrasion.

The above enhancement in superhydrophobicity and mechanical robustness for the PE-SNF film after annealing is ascribed to the induced hierarchical micro/nanoscale surface structures as well as the enhanced adhesion between silicon layer and the base layer of PE film. This is evidently revealed by the SEM results, as shown in Figure 4. After 30 cycles tape-peeling, the SNF layer

was totally removed and the silicon layer was partially peeled off from the unannealed PE-SNF film surface (see Figure 4a-b). A similar situation was observed for the PE-SNF film surface after 20 cycles abrasion (Figure 4e-f). This well explains the mechanical susceptibility of the superhydrophobicity for the PE-SNF without annealing. In contrast to the unannealed PE-SNF, the SNF was mostly retained on the PE-SNF-A after either 30 cycles tape-peeing (Figure 4 c-d) or 20 cycles of abrasion (Figure 4g-h). Only those areas exposed to the tape-peeling or abrasive forces (Figure 4c-d, g-h and Figure 3c) showed signs of the damaged SNF texture, while the majority of the SNF were protected by the micro-wrinkled structures. Strikingly, despite of the damaged SNF, the hydrophobic silicone layer remained adhering to the PE micro-wrinkles even after exposed to tape-peeling or adhesion (see Figure 4c-d and 4g-h). The retained hydrophobic silicone layer along with the micro-wrinkled roughness as well as the residual SNF maintained the superhydrophobicity of the PE-SNF-A film. This well explains the mechanically robust superhydrophobicity of the PE-SNF film after thermal annealing. The robust superhydrophobicity also indicates a durable self-cleaning functionality of the as-prepared PE-SNF-A film.

To further explore the stability of the superhydrophobicity for the obtained PE-SNF-A film, a water droplet (10 μL) was placed on the film surface, as shown in Figure 5a. When the droplet gradually shrank due to the evaporation, it kept nearly spherical shape and the Θ_{CA} was maintained higher than 150° during the whole 84 min evaporation process (Figure 5a). This reveals that the as-prepared PE-SNF-A film can prevent even a very tiny sized water droplet from permeating into it, indicating a very stable superhydrophobicity. Moreover, when exposed to a ~90% humidity condition, the as-prepared PE-SNF-A film maintained Θ_{CA} and Θ_{SA} of ~ 170° and ~ 3°, respectively, during the whole process (Figure 5b). After 16 days exposure, no observable decrease in Θ_{CA} or increase in Θ_{SA}, suggesting a rather durable resistance of the superhydrophobicity to the

high humidity environment. In addition, the obtained PE-SNF-A film exhibited excellent repellency to highly corrosive liquids. As shown in Figure 5c, all the corrosive liquid droplets varied from strong acid (pH 1) to strong base (pH 14) featured Θ_{CA} above 165° and Θ_{SA} below 5° on the PE-SNF-A film surface.

To further assess the resistance of the superhydrophobicity to harsh chemical corrosions, the as-prepared PE-SNF-A films were immersed in 0.1 M hydrochloric acid (HCl) and 0.1 M sodium hydroxide (NaOH) solutions, and the Θ_{CA} and Θ_{SA} of the film as a function of corrosion time were measured. Figure 5d and e show the influence of corrosion time on Θ_{CA} and Θ_{SA} of the PE-SNF-A film in HCl and NaOH solutions, respectively.

Strikingly, even after 2 hours HCl corrosion, the as-prepared film showed excellent superhydrophobicity featuring Θ_{CA} and Θ_{SA} of ~ 169° and 9°, respectively (see Figure 5d). The PE-SNF-A film also maintained the Θ_{CA} of ~ 163° and Θ_{SA} of ~ 15° after 30 min corrosion in NaOH (see Figure 5e). The increase in Θ_{SA} of the as-prepared film after NaOH/HCl corrosion is ascribed to the hydrolysis of the surface area that contacted with the corrosive liquids. SEM images of the PE-SNF-A surface show no observable damage after HCl and NaOH corrosion, as shown in Figure 5g and h, respectively. Furthermore, in contrast to the widely reported superhydrophobic surfaces prepared by spray coatings,[42, 50] the as-prepared PE-SNF-A film even exhibited rather stable superhydrophobicity to organic solvents, *e.g.*, dimethylformamide (DMF), tetrahydrofuran (THF), toluene, etc. As shown in Figure 5f, the PE-SNF-A film maintained its excellent water repellency with a Θ_{CA} of ~ 170° and Θ_{SA} of ~ 3° after 4 days immersion in these aggressive organic solvents, and no observable damage from the film surface was found (see Figure 5i and Figure S3). In addition, the as-prepared superhydrophobic film also shows excellent resistance towards UV

irradiation, for instance, after 24 h UV light illumination no obvious change was found for the Θ_{CA} and Θ_{SA} of the PE-SNF-A film (see Figure S4).

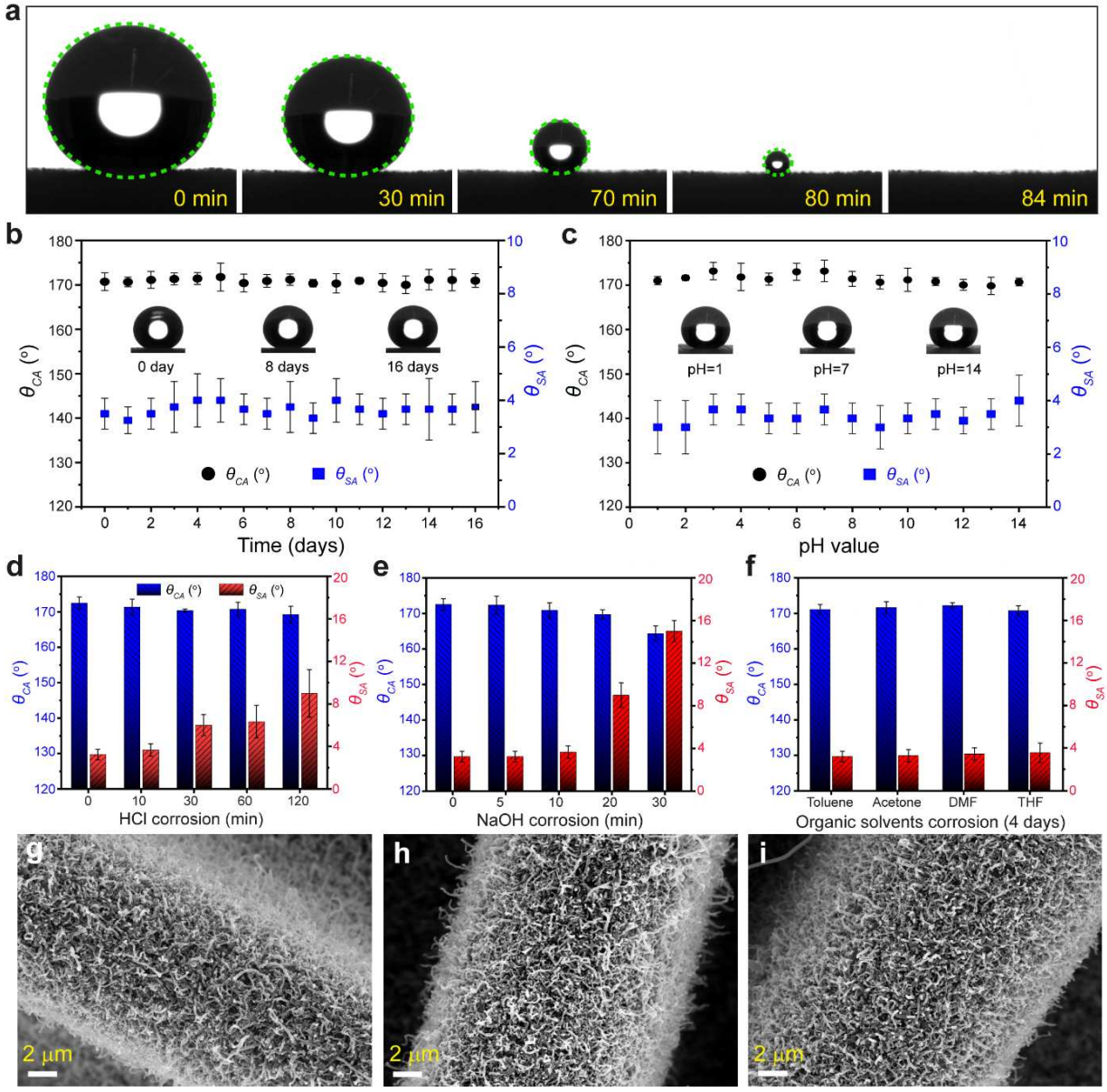

Figure 5. (a) A 10 μL water droplet placed on the PE-SNF-A film gradually shrank with time due to the evaporation. The droplet maintained its perfect spherical shape with Θ_{CA} greater than 150° in the whole process. (b) Θ_{CA} and Θ_{SA} of the as-prepared PE-SNF-A film as a function of time after exposed to a ~ 90% humidity condition. (c) Θ_{CA} and Θ_{SA} of corrosive liquids with pH values

vary from 1 to 14. Influence of (d) HCl and (e) NaOH solution corrosion time on the water repellency of the PE-SNF-A film. Both the HCl and NaOH solution used feature a concentration of 0.1 M. (f) Θ_{CA} and Θ_{SA} of the PE-SNF-A film after 4 days corrosion in different organic solvents. SEM images of the PE-SNF-A film surface after (g) 120 min corrosion in 0.1M HCl solution and (h) 30 min corrosion in 0.1 M NaOH solution, as well as (i) 4 days corrosion in dimethylformamide (DMF).

Such stable superhydrophobicity and excellent resistance to chemical corrosions of the as-prepared PE-SNF-A film are ascribed to the synergistic effect of the inherent chemical stability of the composite film with the hierarchical micro/nanoscale surface structures. The formed dual-scale air pockets resulting from the trapped air within the micro/nanoscopic structure (Figure 3a), prevented the water droplets and corrosive liquids from seeping through the film.

The as-prepared PE-SNF-A film not only shows excellent water repellency, but also exhibits non-wettability to the other aqueous solutions such as, soy sauce, coffee, wine, milk and cola (see Figure 6a). Due to its robust superhydrophobicity, the PE-SNF-A film features excellent self-cleaning functionality. Figure 6b-c demonstrates the self-cleaning effect of the film using chalk powder as the mimic dirt. The film was quickly and completely cleaned when water droplets were poured onto its surface as the dirt was picked up and taken away by the rolling droplets.

Notably, the self-cleaning property of the as-prepared film also functions after oil contamination when exposed to either air or oil. Figure 6d shows a water droplet forming a sphere and rolling off from the oil (hexadecane) immersed film surface instead of wetting or adhering on the surface, which suggests that the film maintained its self-cleaning functionality even when exposed to oil. In addition, the water droplets can easily slip off from the oil contaminated film surface when exposed to air (see Figure 6e-f and Movie S3). Figure 6g-i show a dirt-removal test

on the PE-SNF-A film surface in both oil and air. The film was fully immersed into oil (hexadecane) followed by partly putting into the oil. The dirt (chalk powder) was also placed partly in oil and air onto the film surface, which was subsequently cleared by water droplets slipped off the surface (Figure 6g-i and Movie S4).

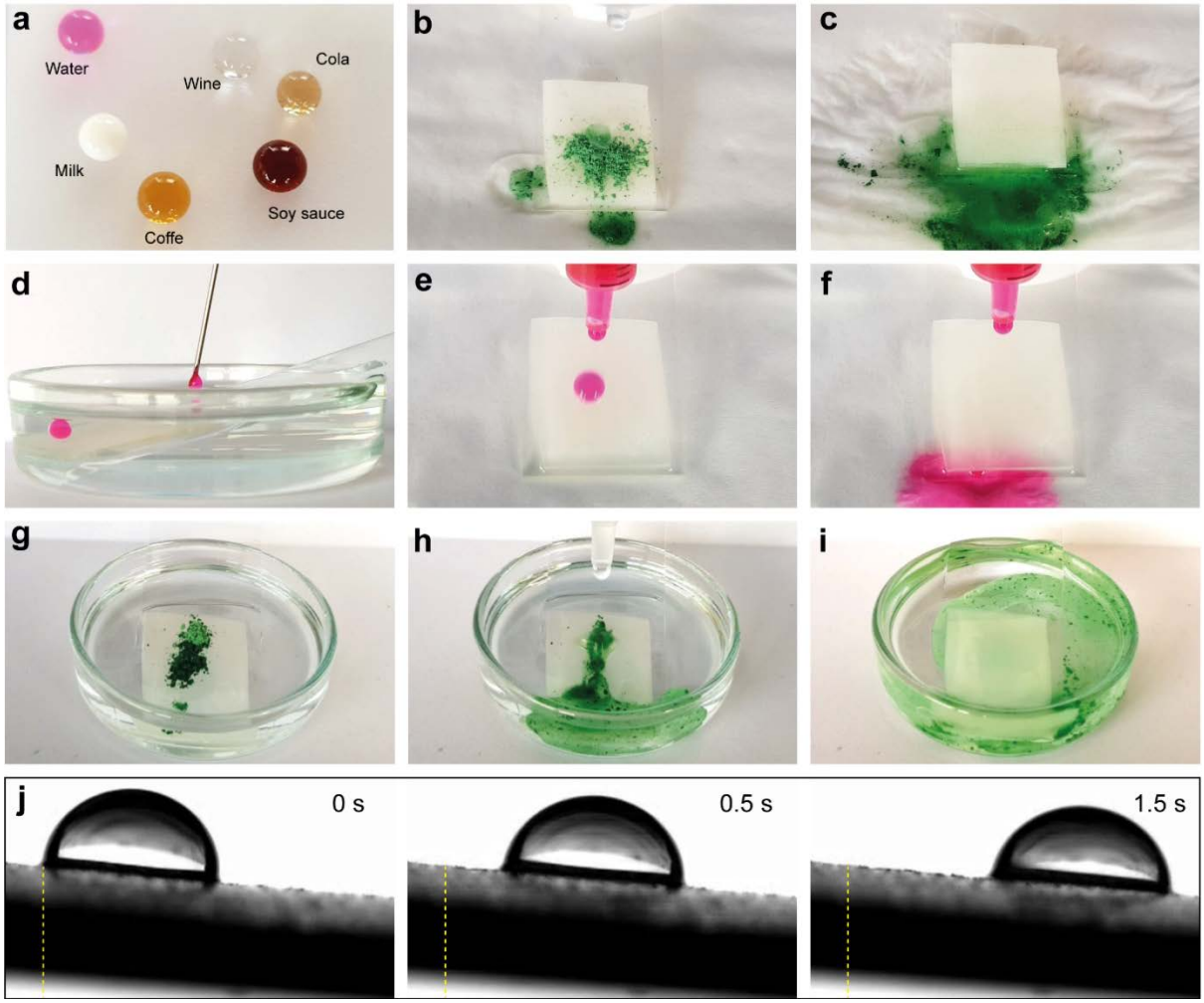

Figure 6. (a) Repellent behavior of PE-SNF-A film when exposed to water, wine, cola, soy sauce, coffee and milk. (b-c) Self-cleaning process on PE-SNF-A film surface when exposed to air. Chalk powder was used as the dirt to contaminate the surface. (d) Water droplet was repelled by the film surface immersed in oil (hexadecane). (e-f) The PE-SNF-A film surface retained its water repellency even after oil contamination. (g-i) Self-cleaning test at solid-oil-vapor interface. The

dirt was partly put in oil and air, subsequently, the dirty was removed by water drops passing over the oil contaminated film surface. (j) Time resolved images showing a water droplet (10 μL) slipping off from the oil contaminated PE-SNF-A film surface under a Weber number[51] of around 10.6.

When the film was immersed in oil, the oil can gradually penetrate through its surface, and the water droplets were supported by both the micro/nanoscale surface structures and oil.[43] This results in the similar water repellency and self-cleaning performance in oil to that in air.[52] In air, after oil immersion, the hierarchical micro/nanoscale surface texture of the film can lock the oil contamination as a lubricating fluid, leading to a slippery state,[53] as shown in Figure 6j. The dirt can be taken away from the film surface by the sliding over water drops. Hence, the oil contaminated film maintains its water repellency and self-cleaning functionality when exposed to either air or oil.

CONCLUSION

In summary, we presented a facial solvent-free technique to fabricate flexible superhydrophobic composite films with novel hierarchical micro/nanoscopic structures and mechanochemically robust superhydrophobicity. The obtained film exhibited very stable superhydrophobicity with water contact angle of ~ 170° and sliding angle of ~ 3°. Notably, the film can maintain its superhydrophobicity under a variety of harsh mechanical and chemical treatments such as, cyclic abrasion, tape-peeling, flexing, knife-cutting, intensive finger-wiping as well as corrosions from strong acid/base solutions. The robust superhydrophobicity is owing to the induced hierarchical micro/nanoscale surface structures, leading to the trapped dual-scale air pockets. In contrast to most superhydrophobic coatings, the as-prepared superhydrophobic composite film also featured excellent resistance towards organic solvents. In addition, even after oil contamination, the

composite film maintained its water repellency and self-cleaning property. The robust water-repellent functionality of the composite film developed here potentially endows its promising and versatile applications in various areas.

EXPERIMENTAL SECTION

Materials. Trichloroethylsilane (TCES, 98%) was purchased from ABCR GmbH (Germany). Low density polyethylene film (LDPE) was purchased from Angst + Pfister (Switzerland). Toluene (99.8%), tetrahydrofuran (THF, ≥ 99.5%), dimethylformamide (DMF, ≥ 99.8%), hydrochloric acid (37%) and sodium hydroxide (≥ 97%) were purchased from Sigma-aldrich. Ethanol and acetone (absolute for analysis) were purchased from Merck Millipore. Milli-Q water was produced by a Millipore Simplicity system (Billerica, MA, USA). Unless otherwise mentioned all other chemicals were used as received.

Sample Preparation. In order to prepare the superhydrophobic composite film, the polyethylene film was first activated by O_2 plasma in a plasma chamber (Diener Electronics, Nagold Germany) at 100-watt power for 10 min under the O_2 flow rate of 10 sccm. Subsequently, the activated film was placed into a custom-built glass desiccator and equilibrated for 2 h under a controlled humidity of 50% ± 2%. The humidity inside the desiccator was monitored by EE23 (E+E Elektronik, Germany) hygrometer and adjusted by using the mixture of dry and humidified N_2. To initial the coating of silicone nanofilaments (SNF) on the activated film, 800 µL TCES was injected into the desiccator and the reaction was conducted at room temperature (~22 °C) for 6 h. The obtained SNF coated film (PE-SNF) was then treated with thermal annealing. To obtain an adequate annealing treatment, the samples were annealed at 180 °C (above the melting point of the PE film) for 10 min to induce the hierarchical micro/nanoscale surface structures. We note that

no obvious change was observed for the surface morphology after a longer period of annealing. In addition, we also performed the SNF coating on PE film surface with different amount of TCES (*i.e.,* 300 μl and 1200 μl). With less amount of TCES (300 μl), the coating of SNF was found to be not homogeneous (see Figure S5a and b), and the coated PE film is not superhydrophobic. After further increase the using amount of TCES to 1200 μl, a similar homogeneous dense layer of SNF was obtained on the PE film surface (see Figure S5c and d) and no obvious change in SNF morphology was found when compared to that of using 800 μl TCES. Thus, in this work we performed all the experiments based on the PE films coated with 800 ul TCES.

Characterizations. A high resolution scanning electron microscope (SEM) combined with energy dispersive X-ray (EDX) (Zeiss Supra 50 VP, German) were used to characterize the composite films surface structures. The typically used electron acceleration voltage was 10 keV. Prior to SEM-EDX analysis the samples were coated with 5 nm layer of platinum. The contact angle and sliding angle measurements were performed using a Contact Angle System OCA (Stuttgart, Germany). An RPR-200 model reactor (SNE Ultraviolet Co., USA) equipped with eight UV lamps (SNE Ultraviolet Co., USA) with emission wavelength at 350 nm was used to assess the UV resistance of the obtained superhydrophobic films. The contact angle and sliding angle of the films after UV light irradiation were measured.

Mechanical Performance Tests. The flexural measurements were performed with an Instron 3345 universal testing device. A three-point bending setup was used. The support span was set to be 30 mm. The typical sample dimensions were 60 mm × 10 mm × 1.2 mm. The applied testing rate was 1 mm min^{-1}. For average values of the maximum stress and strain, at least three specimens were measured.

Tape-peeling Test. An adhesive tape (3M, Scotch® Magic™ Tape 810) with adhesion force of 250 N m^{-1} to steel (ASTM D-3330) was used for the tape-peeling test. The tape was placed and pressed with a load of 900 g on the prepared composite film to achieve uniform contact between the tape and the film, followed by slowly peeling the tape away from the film surface. The contact angles and sliding angles of the tape-peeled substrates were investigated as a function of tape-peeling cycles.

Abrasion Test. The mechanical abrasion tests were conducted using AB5000 Washability Tester (TQC, Germany). ASTM standard D4213 for testing abrasion or scrub resistance of coatings and paints was adapted to assess the abrasion resistance of the as-prepared composite film. The friction partner was mounted on a reciprocating sled which oscillates with a given stroke speed. The applied load, stroke speed and distance were 200 g, 10 cycles min^{-1} and 30 cm, respectively. The contact angles and sliding angles of the abraded films were measured as a function of abrasion cycles.

ASSOCIATED CONTENT

Supporting Information.

The Supporting Information is available free of charge on ACS Publications website.

SEM images of LDPE films before and after annealing treatment. Flexural measurement of the PE-SNF film without annealing. SEM images of the PE-SNF-A film surface after 4 days corrosion in tetrahydrofuran, acetone and toluene. Speeded up movies showing finger wiping, cyclic flexing and knife-cutting tests performed on PE-SNF-A film (Movie 1, mp4) and PE-SNF film without annealing (Movie 2, mp4). Speeded up movies showing the water repellent behavior of PE-SNF-

A film after oil contamination (Movie 3, mp4) and the self-cleaning performance of PE-SNF-A film in either oil or air (Movie 4, mp4).

AUTHOR INFORMATION

Corresponding Author

* Email: sseeger@chem.uzh.ch

Author Contributions

The manuscript was written through contributions of all authors. All authors have given approval to the final version of the manuscript. ‡These authors contributed equally.

ACKNOWLEDGMENT

The authors acknowledge the Center for Microscopy and Image Analysis (ZMB) of University of Zurich for giving the access to the microscopic facilities.

REFERENCES

(1) Fürstner, R.; Barthlott, W.; Neinhuis, C.; Walzel, P., Wetting and Self-Cleaning Properties of Artificial Superhydrophobic Surfaces. *Langmuir* **2005,** *21*, 956-961.

(2) Min, W.-L.; Jiang, B.; Jiang, P., Bioinspired Self-Cleaning Antireflection Coatings. *Adv. Mater.* **2008,** *20*, 3914-3918.

(3) Zhang, X.; Liu, S.; Salim, A.; Seeger, S., Hierarchical Structured Multifunctional Self-Cleaning Material with Durable Superhydrophobicity and Photocatalytic Functionalities. *Small* **2019,** *15*, 1901822.

(4) Wang, Y.; Gong, X., Superhydrophobic Coatings with Periodic Ring Structured Patterns for Self-Cleaning and Oil–Water Separation. *Adv. Mater. Interfaces* **2017**, *4*, 1700190.

(5) Peng, J.; Zhao, X.; Wang, W.; Gong, X., Durable Self-Cleaning Surfaces with Superhydrophobic and Highly Oleophobic Properties. *Langmuir* **2019**, *35*, 8404-8412.

(6) Lu, Y.; Sathasivam, S.; Song, J.; Chen, F.; Xu, W.; Carmalt, C. J.; Parkin, I. P., Creating Superhydrophobic Mild Steel Surfaces for Water Proofing and Oil–water Separation. *J. Mater. Chem. A* **2014,** *2*, 11628-11634.

(7) Wang, L.; Gong, Q.; Zhan, S.; Jiang, L.; Zheng, Y., Robust Anti-Icing Performance of a Flexible Superhydrophobic Surface. *Adv. Mater.* **2016,** *28*, 7729-7735.

(8) Zang, D.; Zhu, R.; Zhang, W.; Yu, X.; Lin, L.; Guo, X.; Liu, M.; Jiang, L., Corrosion-Resistant Superhydrophobic Coatings on Mg Alloy Surfaces Inspired by Lotus Seedpod. *Adv. Funct. Mater.* **2017,** *27*, 1605446.

(9) Tripathy, A.; Kumar, A.; Sreedharan, S.; Muralidharan, G.; Pramanik, A.; Nandi, D.; Sen, P., Fabrication of Low-Cost Flexible Superhydrophobic Antibacterial Surface with Dual-Scale Roughness. *ACS Biomater. Sci. Eng.* **2018,** *4*, 2213-2223.

(10) Wu, M.; Ma, B.; Pan, T.; Chen, S.; Sun, J., Silver-Nanoparticle-Colored Cotton Fabrics with Tunable Colors and Durable Antibacterial and Self-Healing Superhydrophobic Properties. *Adv. Funct. Mater.* **2016,** *26*, 569-576.

(11) Yohe, S. T.; Colson, Y. L.; Grinstaff, M. W., Superhydrophobic Materials for Tunable Drug Release: Using Displacement of Air To Control Delivery Rates. *J. Am. Chem. Soc.* **2012,** *134*, 2016-2019.

(12) Falde, E. J.; Yohe, S. T.; Colson, Y. L.; Grinstaff, M. W., Superhydrophobic Materials for Biomedical Applications. *Biomaterials* **2016,** *104*, 87-103.

(13) Feng, L.; Zhang, Z.; Mai, Z.; Ma, Y.; Liu, B.; Jiang, L.; Zhu, D., A Super-Hydrophobic and Super-Oleophilic Coating Mesh Film for the Separation of Oil and Water. *Angew. Chem.* **2004,** *116*, 2046-2048.

(14) Crick, C. R.; Gibbins, J. A.; Parkin, I. P., Superhydrophobic Polymer-coated Copper-mesh; Membranes for Highly Efficient Oil–water Separation. *J. Mater. Chem. A* **2013,** *1*, 5943-5948.

(15) Zhou, X.; Zhang, Z.; Xu, X.; Guo, F.; Zhu, X.; Men, X.; Ge, B., Robust and Durable Superhydrophobic Cotton Fabrics for Oil/Water Separation. *ACS Appl. Mater. Interfaces* **2013,** *5*, 7208-7214.

(16) Chu, Z.; Feng, Y.; Seeger, S., Oil/Water Separation with Selective Superantiwetting/Superwetting Surface Materials. *Angew. Chem. Int. Edit.* **2015,** *54*, 2328-2338.

(17) Wang, Y.; Gong, X., Special Oleophobic and Hydrophilic Surfaces: Approaches, Mechanisms, and Applications. *J. Mater. Chem. A* **2017**, *5*, 3759-3773.

(18) Li, J.; Xu, C.; Guo, C.; Tian, H.; Zha, F.; Guo, L., Underoil Superhydrophilic Desert Sand Layer for Efficient Gravity-directed Water-in-oil Emulsions Separation with High Flux. *J. Mater. Chem. A* **2018**, *6*, 223-230.

(19) Gao, S.; Tang, G.; Hua, D.; Xiong, R.; Han, J.; Jiang, S.; Zhang, Q.; Huang, C., Stimuli-responsive Bio-based Polymeric Systems and Their Applications. *J. Mater. Chem. B* **2019**, *7*, 709-729.

(20) Zhang, P.; Zhao, C.; Zhao, T.; Liu, M.; Jiang, L., Recent Advances in Bioinspired Gel Surfaces with Superwettability and Special Adhesion. *Adv. Sci.* **2019**, *6*, 1900996.

(21) Gao, S.; Huang, J.; Li, S.; Liu, H.; Li, F.; Li, Y.; Chen, G.; Lai, Y., Facile Construction of Robust Fluorine-free Superhydrophobic TiO2@fabrics with Excellent Anti-fouling, Water-oil Separation and UV-Protective Properties. *Mater. Design* **2017**, *128*, 1-8.

(22) Cottin-Bizonne, C.; Barrat, J.-L.; Bocquet, L.; Charlaix, E., Low-friction Flows of Liquid at Nanopatterned Interfaces. *Nat. Mater.* **2003,** *2*, 237-240.

(23) Song, M.; Hu, D.; Zheng, X.; Wang, L.; Yu, Z.; An, W.; Na, R.; Li, C.; Li, N.; Lu, Z.; Dong, Z.; Wang, Y.; Jiang, L., Enhancing Droplet Deposition on Wired and Curved Superhydrophobic Leaves. *ACS Nano* **2019**, *13*, 7966-7974.

(24) Li, Z.; Cao, M.; Li, P.; Zhao, Y.; Bai, H.; Wu, Y.; Jiang, L., Surface-Embedding of Functional Micro-/Nanoparticles for Achieving Versatile Superhydrophobic Interfaces. *Matter* **2019**, *1*, 661-673.

(25) Ben, S.; Zhou, T.; Ma, H.; Yao, J.; Ning, Y.; Tian, D.; Liu, K.; Jiang, L., Multifunctional Magnetocontrollable Superwettable-Microcilia Surface for Directional Droplet Manipulation. *Adv. Sci.* **2019**, *6*, 1900834.

(26) Wang, Y.; Lai, H.; Cheng, Z.; Zhang, H.; Liu, Y.; Jiang, L., Smart Superhydrophobic Shape Memory Adhesive Surface toward Selective Capture/Release of Microdroplets. *ACS Appl. Mater. Interfaces* **2019**, *11*, 10988-10997.

(27) Dong, S.; Li, Y.; Tian, N.; Li, B.; Yang, Y.; Li, L.; Zhang, J., Scalable Preparation of Superamphiphobic Coatings with Ultralow Sliding Angles and High Liquid Impact Resistance. *ACS Appl. Mater. Interfaces* **2018,** *10*, 41878-41882.

(28) Zhang, J.; Seeger, S., Superoleophobic Coatings with Ultralow Sliding Angles Based on Silicone Nanofilaments. *Angew. Chem. Int. Edit.* **2011,** *50*, 6652-6656.

(29) Zhang, J.; Seeger, S., Silica/Silicone Nanofilament Hybrid Coatings with Almost Perfect Superhydrophobicity. *ChemPhysChem* **2013,** *14*, 1646-1651.

(30) Artus, G. R. J.; Jung, S.; Zimmermann, J.; Gautschi, H.-P.; Marquardt, K.; Seeger, S., Silicone Nanofilaments and Their Application as Superhydrophobic Coatings. *Adv. Mater.* **2006,** *18*, 2758-2762.

(31) Wang, P.; Zhao, T.; Bian, R.; Wang, G.; Liu, H., Robust Superhydrophobic Carbon Nanotube Film with Lotus Leaf Mimetic Multiscale Hierarchical Structures. *ACS Nano* **2017,** *11*, 12385-12391.

(32) Shiu, J.-Y.; Kuo, C.-W.; Chen, P.; Mou, C.-Y., Fabrication of Tunable Superhydrophobic Surfaces by Nanosphere Lithography. *Chem. Mater.* **2004,** *16*, 561-564.

(33) Qian, B.; Shen, Z., Fabrication of Superhydrophobic Surfaces by Dislocation-Selective Chemical Etching on Aluminum, Copper, and Zinc Substrates. *Langmuir* **2005,** *21*, 9007-9009.

(34) Cheng, Y.; Zhu, T.; Li, S.; Huang, J.; Mao, J.; Yang, H.; Gao, S.; Chen, Z.; Lai, Y., A Novel Strategy for Fabricating Robust Superhydrophobic Fabrics by Environmentally-friendly Enzyme Etching. *Chem. Eng. J.* **2019**, *355*, 290-298.

(35) Han, J.; Yue, Y.; Wu, Q.; Huang, C.; Pan, H.; Zhan, X.; Mei, C.; Xu, X., Effects of Nanocellulose on the Structure and Properties of Poly(vinyl alcohol)-borax Hybrid Foams. *Cellulose* **2017**, *24*, 4433-4448.

(36) Gong, X.; Wang, Y.; Kuang, T., ZIF-8-Based Membranes for Carbon Dioxide Capture and Separation. *ACS Sustain. Chem. Eng.* **2017**, *5*, 11204-11214.

(37) Chu, Z.; Seeger, S., Superamphiphobic Surfaces. *Chem. Soc. Rev.* **2014,** *43*, 2784-2798.

(38) Verho, T.; Bower, C.; Andrew, P.; Franssila, S.; Ikkala, O.; Ras, R. H. A., Mechanically Durable Superhydrophobic Surfaces. *Adv. Mater.* **2011,** *23*, 673-678.

(39) Gong, D.; Long, J.; Jiang, D.; Fan, P.; Zhang, H.; Li, L.; Zhong, M., Robust and Stable Transparent Superhydrophobic Polydimethylsiloxane Films by Duplicating via a Femtosecond Laser-Ablated Template. *ACS Appl. Mater. Interfaces* **2016,** *8*, 17511-17518.

(40) Tan, J.; Hao, J.; An, Z.; Liu, C., Superhydrophobic Surfaces on Brass Substrates Fabricated via Micro-etching and a Growth Process. *RSC Adv.* **2017,** *7*, 26145-26152.

(41) Wang, N.; Xiong, D.; Deng, Y.; Shi, Y.; Wang, K., Mechanically Robust Superhydrophobic Steel Surface with Anti-Icing, UV-Durability, and Corrosion Resistance Properties. *ACS Appl. Mater. Interfaces* **2015,** *7*, 6260-6272.

(42) Peng, C.; Chen, Z.; Tiwari, M. K., All-organic Superhydrophobic Coatings with Mechanochemical Robustness and Liquid Impalement Resistance. *Nat. Mater.* **2018,** *17*, 355-360.

(43) Lu, Y.; Sathasivam, S.; Song, J.; Crick, C. R.; Carmalt, C. J.; Parkin, I. P., Robust Self-cleaning Surfaces That Function When Exposed to Either Air or Oil. *Science* **2015,** *347*, 1132-1135.

(44) Artus, G. R. J.; Olveira, S.; Patra, D.; Seeger, S., Directed In Situ Shaping of Complex Nano- and Microstructures during Chemical Synthesis. *Macromol. Rapid Commun.* **2017,** *38*, 1600558.

(45) James, M.; Darwish, T. A.; Ciampi, S.; Sylvester, S. O.; Zhang, Z.; Ng, A.; Gooding, J. J.; Hanley, T. L., Nanoscale Condensation of Water on Self-assembled Monolayers. *Soft Matter* **2011**, *7*, 5309-5318.

(46) Cao, P.; Xu, K.; Varghese, J. O.; Heath, J. R., The Microscopic Structure of Adsorbed Water on Hydrophobic Surfaces under Ambient Conditions. *Nano Letters* **2011**, *11*, 5581-5586.

(47) Ware, C. S.; Smith-Palmer, T.; Peppou-Chapman, S.; Scarratt, L. R. J.; Humphries, E. M.; Balzer, D.; Neto, C., Marine Antifouling Behavior of Lubricant-Infused Nanowrinkled Polymeric Surfaces. *ACS Appl. Mater. Interfaces* **2018,** *10*, 4173-4182.

(48) Scarratt, L. R. J.; Hoatson, B. S.; Wood, E. S.; Hawkett, B. S.; Neto, C., Durable Superhydrophobic Surfaces via Spontaneous Wrinkling of Teflon AF. *ACS Appl. Mater. Interfaces* **2016,** *8*, 6743-6750.

(49) Saddiqi, N.-u.-H.; Seeger, S., Chemically Resistant, Electric Conductive, and Superhydrophobic Coatings. *Adv. Mater. Interfaces* ***2019,*** *6*, 1900041.

(50) Das, A.; Deka, J.; Raidongia, K.; Manna, U., Robust and Self-Healable Bulk-Superhydrophobic Polymeric Coating. *Chem. Mater.* **2017,** *29*, 8720-8728.

(51) Hao, C.; Li, J.; Liu, Y.; Zhou, X.; Liu, Y.; Liu, R.; Che, L.; Zhou, W.; Sun, D.; Li, L.; Xu, L.; Wang, Z., Superhydrophobic-like Tunable Droplet Bouncing on Slippery Liquid Interfaces. *Nat. Commun.* **2015**, *6*, 7986.

(52) Bhushan, B.; Jung, Y. C.; Koch, K., Self-Cleaning Efficiency of Artificial Superhydrophobic Surfaces. *Langmuir* **2009,** *25*, 3240-3248.

(53) Wong, T.-S.; Kang, S. H.; Tang, S. K. Y.; Smythe, E. J.; Hatton, B. D.; Grinthal, A.; Aizenberg, J., Bioinspired Self-repairing Slippery Surfaces with Pressure-stable Omniphobicity. *Nature* **2011,** *477*, 443-447.